Tellus (1997), 49A, 139–160
Printed in UK – all rights reserved

TELLUS
ISSN 0280–6495

The ICES-boxes approach in relation to results of a North Sea circulation model

By HERMANN-J. LENHART* and THOMAS POHLMANN *Institut für Meereskunde der Universität Hamburg, Troplowitzstr. 7, D-22529 Hamburg, Germany*

(Manuscript received 13 July 1995; in final form 20 June 1996)

ABSTRACT

Based on the division of the North Sea into the ICES boxes, often used as a tool to present data aggregated from measurements, the results of a 3-D baroclinic model for 11 years of simulation are presented. Since the information on the ICES boxes from the 3-D model is available as synoptic property, a comprehensive description of the water budget, the transport through the boxes as well as the flushing times is attained. Moreover, the results of the 3-D model allows for a quantification of the horizontal diffusion acting between the ICES boxes. Integrated properties of the boxes are obtained from comparing the depth of the thermocline derived by vertical diffusion and by the gradient in the temperature profile. Considerable changes can be observed for the period of stratification within the boxes from the gradient in the temperature profile compared to potential energy calculations. The properties of the ICES boxes as the basis for a box model are presented by means of the ecosystem model ERSEM. A tracer study, using freshwater as a conservative tracer, compares the results of the ERSEM box model with the results aggregated from a gridded dispersion model, using the same physical forcing. From this comparison, an appropriate transport representation for the box model is derived. Furthermore the results of ERSEM demonstrate that a modification of the boxes, i.e., by introducing a vertical separation for those boxes which are stratified in summer, can improve the representation of the biological processes influenced by the thermocline dynamics.

1. Introduction

The division of the North Sea introduced by the ICES Comittee (ICES, 1983) is used in a variety of applications as a tool to characterize different regions of the North Sea, like the Quality Status Report of the North Sea (North Sea Task Force, 1993) or the presentation of the NERC North Sea Project by Howarth et al. (1994). Recently, budgets for nutrients (Radach et al., 1990; Radach, 1992) or chemical compounds like cadmium (Kühn et al., 1992) have been calculated in order to get first estimates of the fluxes between the boxes and/or source and sink properties within the boxes. For testing the results of a 3-D model against measurements of a passive tracer like Caesium 137 Backhaus (1984) and Pohlmann et al. (1987) used the boxes to aggregate both the model results and the field data.

Based on the modified ICES boxes the ERSEM (European Regional Seas Ecosystem Model) (Baretta et al., 1995) makes use of the regional differentiation by means of a box model. This comprehensive ecosystem model simulates the large-scale cycling of carbon, oxygen and the macro-nutrients N, P and Si over the seasonal cycle in the North Sea. The water flow and the transport of matter from box to box are calculated by utilizing the results of the 3-D baroclinic model by Pohlmann (1991). Because a large set of validation data for the years 1988 and 1989 from the NERC (Natural Environmental Research

* Corresponding author.

Council) North Sea Project and from other sources were available, we forced ERSEM with results from the circulation model for these two years.

In the process of providing the hydrodynamical forcing for ERSEM, we first had to review the hydrodynamical ICES box characteristics by using the results of the circulation model. Since information on the ICES boxes is available from the circulation model (Pohlmann, 1996a) as synoptic properties, a comprehensive information, e.g., on the water budget, the transport through the boxes as well as the flushing times will be given. Also values for horizontal diffusion between the boxes could be obtained from the circulation model, which was not achieved by the flushing times report (ICES, 1983). Furthermore, integrated properties like the mixed layer depth as sub-scale properties within the ICES boxes were derived.

The last part of the paper covers the question of how well the ICES boxes can be used as the structural setup for a box model. Different representations of the transport were tested against the aggregated results from a 3-D advection-diffusion (AD) model (Pohlmann, 1991) for a conservative tracer. Especially the role of numerical diffusion at work within the boxes has to be outlined. Finally, the effect of the vertical diffusion on the nutrient dynamics as simulated in ERSEM will be presented. This was done in view of a modification of the ICES boxes for the use in ERSEM by introducing a vertical separation at 30 m depth for the deep boxes of the central and northern North Sea, where thermal stratification occurs regularly in summer.

2. The grid cell model

2.1. The circulation model

The model applied in the current investigation is a modified version of the shelf sea circulation model developed by Backhaus (1983). The governing equations are the shallow water equations in combination with the hydrostatic assumption, the equation of continuity, the transport equations for temperature and salinity and the equation of state for sea water. A complete discussion of the semi-implicit numerical scheme, which is used to solve this system of differential equations is presented in Backhaus (1985). The vertical eddy viscosity is calculated by means of a second order turbulent closure scheme originally proposed by Kochergin (1987) and its implementation further discussed in Pohlmann (1996b).

This model has extensively been applied in particular to the North Sea region (cf. Backhaus and Hainbucher, 1987; Hainbucher et al., 1987). Thus, the general ability of the model to reproduce the hydrodynamic conditions of the North Sea has been proven.

The North Sea model by Pohlmann (1991) was used to prognostically calculate the following hydrodynamic parameters: sea level ζ, velocities u, v, w, temperature T, salinity S, density ρ and vertical eddy viscosity A_v for the period from 1 January 1982 to 31 December 1992 continuously in the domain shown in Fig. 1. Over this period the model was driven by three-hourly wind and atmospheric pressure distributions, which are produced on a grid of 42 km by means of an objective analysis of ship observations (Luthardt, 1987) and by daily sea surface temperatures, provided by the Bundesamt für Seeschiffahrt und Hydrographie (Becker et al., 1984). These SST data are prescribed in the first model layer, i.e., a Dirichlet boundary condition is used for temperature at the sea surface. Since the first model layer has an average thickness of 5 m, this implies that all the solar radiation is absorbed in the upper 5 m of the water column, which introduces an error of the order of 5% in this relatively turbid shelf sea.

At the open boundaries salinity and temperature as well as sea level elevations were prescribed. Salinity and temperature data were prescribed as climatological monthly means, which were calculated from observational data covering the period from 1968 to 1985 (Damm, 1989). The sea level elevations were provided by a 3-D diagnostic baroclinic model covering the entire northwest European continental shelf in order to include all the major remote field effects like external surges.

The horizontal resolution of the North Sea model is 12′ in meridional and 20′ in zonal direction. The discretisation and the underlying topography of the model domain is given in Fig. 1. In the vertical a maximum of 19 layers is defined. This is necessary for an adequate resolution of that part of the water column which is influenced by a thermocline; the thickness of the upper 10 layers is 5 m. The thickness of the lower layers

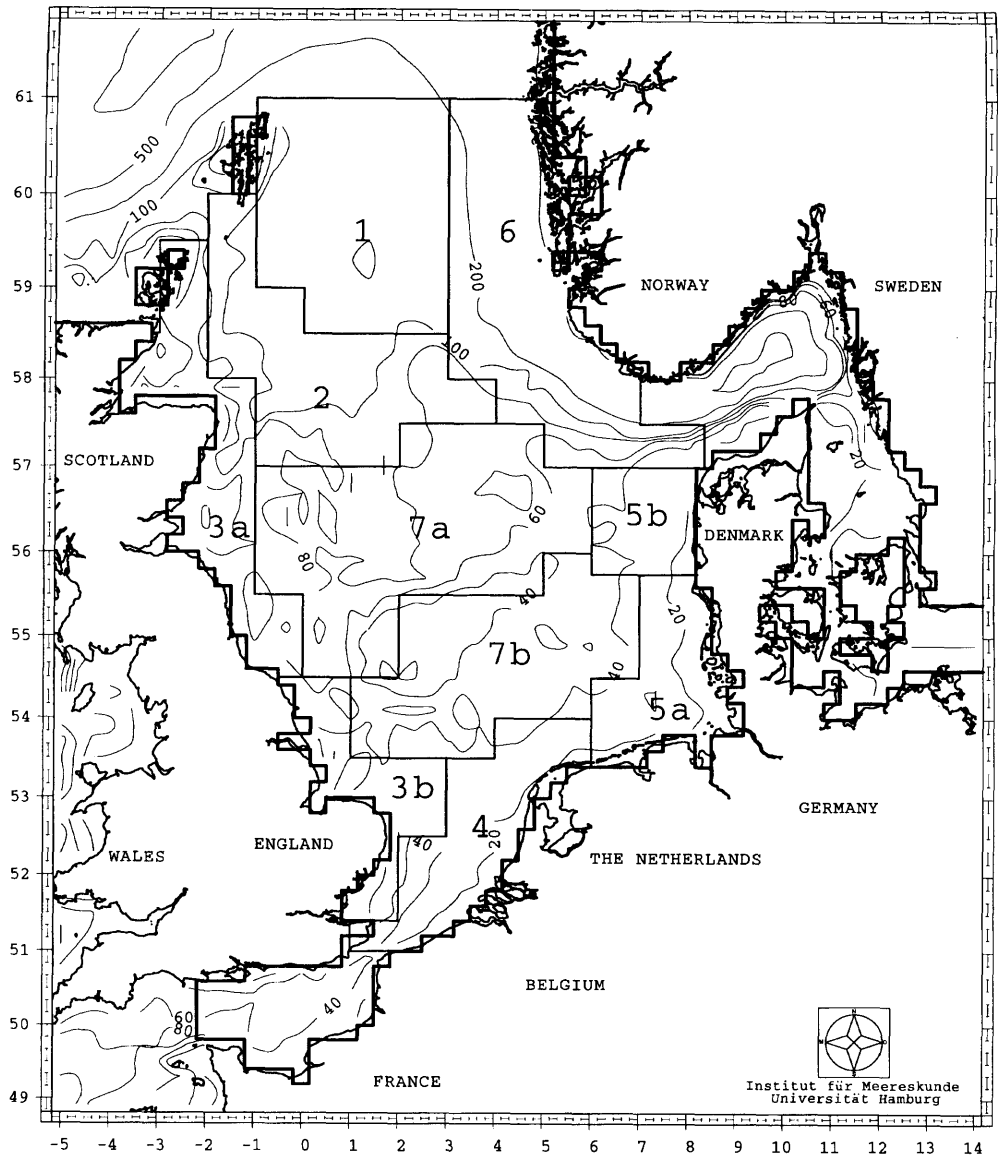

Fig. 1. Model domain and discretization of the gridded model with underlaying topogrophy represented in m and the modified ICES box division of the North Sea as used in this paper.

gradually increases from 10 to 400 m with increasing depth. The time step is chosen to be 20 min, which turns out to be sufficient for a reasonable resolution of all major processes induced by the M_2-tide, which defines the highest frequency of importance on the space-time scales under consideration.

The output of the model comprises values averaged over two tidal cycles. By this means the M_2 tide was filtered out. In order to provide also information on processes occurring on time scales smaller than one day, additionally the variances of the velocities σ_u^2 and σ_v^2 were stored in order to render possible the calculation of the horizontal

eddy viscosity A_h. As the tidal mixing is only important on spatial scales of the order of the tidal excursion, it is of minor importance for large scale North Sea models. Therefore only the principle effect of the tidal mixing needs to be taken into account. This means that neglecting neap-spring variations does not impose a severe limitation to the results of this study. For analogous reasons the influence of high frequency fluctuations of the wind forcing on dispersion processes can be omitted. Especially because the daily mean effect of these fluctuations on the thermocline depth and the vertical diffusion coefficient is included in the daily mean values, as the circulation model is forced by actual, 3-hourly wind fields.

2.2. *The dispersion model*

In the dispersion model concentration of matter is calculated by means of an advection-diffusion equation, which is solved explicitly. The advective terms are determined with help of the velocity field and the vertical diffusion is simulated by using the stored distribution of A_v. According to Maier-Reimer and Sündermann (1982) the horizontal diffusion coefficients A_h are calculated according to:

$$A_h = 0.5\ \sigma^2_{<u,v>}\ \mathrm{d}t \qquad (1)$$

where $\mathrm{d}t$ is the effective diffusion time, which according to Van Dam (1994) can be set to half the M_2 tidal period, if the tide is the dominant signal as it is in the North Sea. This approach implies that most of the diffusion results from the sub-grid tidal excursion of the M_2 tide on a time scale between 24 h and 20 min, ie. the time step of the circulation model. Since the S_2 tide only contributes at the most 30% to the total tidal velocities this possible range should be kept in mind when the the horizontal eddy viscosities are discussed. Moreover, due to the relatively coarse resolution of the circulation model it can not be expected that frontal zones are resolved adequately. This means that it is not sensible to include the effect of stratification on the A_h formulation.

To circumvent problems with different grids the spatial resolution of the dispersion model is chosen to be the same as the resolution of the circulation model. The time step is two hours, which turned out to be sufficient because the high frequency tidal processes have already been filtered out, as the output of the circulation model comprises values averaged over two tidal cycles. For this reason it is possible to calculate the advection terms with an explicit component-upstream scheme, while the vertical diffusion is still treated implicitly in order to evade the time-restrictive stability criteria for the diffusion equation. Due to the comparably large horizonal grid distances an explicit approach can be used to solve the horizontal diffusion term. As discussed in Prandle (1984) the large artifical diffusion produced by this first order advection scheme (Roache, 1972) can be reduced to an acceptable level by the procedure carried out in this study, ie. operating the dispersion model with the residual velocity field. Further details of the dispersion model are given in Pohlmann (1991).

3. Subdivision of the North Sea into hydrographical regions

The ICES study group on flushing times of the North Sea (ICES, 1983) worked out a division of the North Sea based on morphological, hydrographic and biological aspects. The seven hydrographical regions given are related to the division given by Laevastu (1963), but the division is orientated along the 1 degree longitude and the 0.5 degree latitude lines. This was done in view of the comparability under statistical aspects. With the box division in connection with flushing times, a new concept was presented for looking at the North Sea as a set of connected individually different subregions. This setup was designed to assess problems like the anthropogenic input of pollutants taking into account the local characteristics of individual boxes as well as the possible exchange between them.

In Fig. 1 the modified ICES box division of the North Sea is also shown over the model topography, as used for this paper. The original ICES box 5 representing the southwest North Sea is split up into two boxes, roughly separating the German (5A) and the Danish coastal region (5B). The numbers are given according to the modified ICES boxes.

4. Properties of the ICES boxes derived by integrating the gridded model results over the box boundaries

The grid of the 3-D hyrodynamical model determines the location of the boundaries for the ICES boxes. The flow across the boundaries of the boxes is calculated from the velocity components integrated over each of the rectangular box boundaries to give the flow perpendicular to this boundary in units of Sverdrups (1 $Sv = 10^6$ m^3 $s^{-1} = 86.4$ km^3 day^{-1}), separately for the inflow and outflow. For further information see Lenhart et al. (1995).

4.1. Water budget for the ICES boxes

In Table 1, the water budget for the ICES boxes are presented for the years 1988 and 1989 as cumulative values for each year. Calculating the net-difference between in- and outflow as percentage of the inflow value yields values between 0.075 and −0.469% for 1988 and for 1989 between 0.009 and −0.423%. The maximum differences between in- and outflow for all simulated years range from 0.201% to −0.658%. Keeping in mind that variations of the sea surface elevation are not accounted for in this budget the results for the two years presented as well as for the total 11 years of simulations can be regarded as well balanced.

In Table 1 the box 6 shows by far the highest values of in- and outflow. This corresponds to the well known circulation pattern wherein the Norwegian Trench region as main outflow for the North Sea combines water from the northern and southern circulation system. Within box 1 and 2 strong in- and outflows can be observed in relation to the Atlantic inflow in the north. The German Bight box 5A clearly has the lowest values, whereas the much smaller Danish coastal box 5B reaches twice the values of box 5A. This matches the fact, that via the Juetland Current the Danish coastal box 5A represents a major outflow for the southern circulation system into the Norwegian Trench box 6. It is interesting to note that the cumulative in- and outflows for box 7A and 7B, i.e., areas of the central North Sea, exceed that for box 4, the Dutch coastal box with the inflow of the English Channel.

The values of the years 1988 and 1989 in Table 1 are well within the range of values occuring during the period from 1982–1992. Only the year 1988 is exceptional in the occurrence of one single minimum value for the inflow into box 6 going along with 4 maximum values, two in the inflow for box 3B and 4 and two in the outflow for box 7B and 3B.

For the whole North Sea the inflow values for 11 years of simulation vary between 95.2 and 857.6 km^3 day^{-1} and the outflow values between 74.4 and 784.7 km^3 day^{-1}, with the highest values occuring in the winter months. The net difference, here described as mean divergent flow for the whole North Sea is 0.5 km^3 day^{-1}, with minimum and maximum values of −259.5 km^3 day^{-1} and

Table 1. *Cumulative inflow and outflow for the years 1988 and 1989 (km^3); differences are presented as percent of inflow*

	1988			1989		
ICES box	in (km^3)	out	dif (%)	in (km^3)	out	dif (%)
1	60892	60969	−0.127	59809	59850	−0.068
2	75356	75385	−0.038	78492	78486	0.009
6	118319	118283	0.030	121976	121865	0.091
7A	60054	60115	−0.101	55553	55596	−0.077
7B	32624	32624	0.002	28453	28444	0.031
3A	31867	31955	−0.279	35529	35602	−0.207
3B	15566	15587	−0.134	13123	13144	−0.164
4	19796	19876	−0.404	16005	16073	−0.423
5A	7570	7606	−0.469	6411	6433	−0.345
5B	14476	14465	0.075	12610	12598	0.091

252.7 km^3 day^{-1}, respectively. Since the mean in- and outflow are 256.5 km^3 day^{-1} and 257.0 km^3 day^{-1}, it can be concluded that the minimum and maximum divergent flow per day is about equal to the mean in- or outflow per day itself. Dividing the values for the minimum and maximum divergent flow by the North Sea area of 525 000 km^2 yields values of -0.49 m and 0.48 m negative or positive surface elevation change. These results for the difference between in- and outflow are in accordance with many authors (Pohlmann and Sündermann, 1994; Maier-Reimer, 1977). Dividing the North Sea volume of 43 000 km^3 by the mean inflow of 256.5 km^3 day^{-1} results in a mean flushing time for the North Sea of about 167 days.

4.2. *Flushing times*

The ICES Commitee (1983) introduced the 'turn-over time' τ_0 according to the definition given by Bolin and Rodhe (1973) as $\tau_0 = V/Q$. With V as the box volume and Q as the inflow into the box, the water mass within an ICES box is assumed to be entirely removed when the time integral of the inflow (or outflow) Q over the external box boundaries equals the box volume V.

In Table 2, estimates for the flushing-times from different investigations are summarized. The flushing times of all the boxes for the 11 years of simulation in Table 2 lie between 2 (box 5B) and 73 (box 3A) days. Box 5B is exceptional, because the box has the smallest volume with 404 km^3 and acts as a transition box for the water flow from the southern circulation system into the Norwegian trench and therefore shows by far the shortest flushing times between 2 and 29 days. The water masses of the German Bight (box 5A) are exchanged within 33 days in the mean and range from 10 to 56 days. The variability of the flushing for each box is considerable. The Scottish coastal box 3A may be flushed within 18 days (minimum) or in up to 73 days (maximum).

In Table 2, flushing times from a 6 months simulation, covering the period from January to June 1979, by Backhaus (1984) are presented. For this model experiment only the extrema of the vertically integrated flow are listed as minimum and maximum values. Using the same atmospheric forcing of 3-hourly wind data it is not surprising that these data are well within the range given by the flushing times calculated from the gridded model runs. An exception is the maximum value in box 6 and the minimum value in box 2, since one would expect the values of the Backhaus (1984) model study of 181 days to lie within the range of extreme events that 11 years of simulation would provide.

The ICES (1983) report on the flushing times of the North Sea gives values in years for flushing times derived from observations. The same data, recalculated in days, are published in the North

Table 2. *Flushing times calculations in comparison with literature*

		Present study model			Backhaus model α		ICES estimate β	Prandle model γ
ICES box	Volume (km^3)	min (days)	max (days)	mean (days)	min (days)	max (days)	mean (days)	mean (days)
1	6345	21	50	38	35	48	142	177
2	5644	14	49	28	9	39	109	156
6	12815	20	57	38	41	61	76	155
7A	6190	19	68	40	32	49	–	192
7B	2770	13	57	34	31	39	547	83
3A	3176	18	73	36	13	41	–	–
3B	1138	10	50	30	15	30	464	–
4	1323	7	49	28	21	29	73	78
5A	602	10	56	33	10*	27*	73*	86*
5B	404	2	29	11				

(α Backhaus (1984), β ICES (1983), γ Prandle (1984))

* Denotes values from studies for box 5, where the boxes 5A and 5B were combined into one single box 5.

Sea Quality Status Report (NSTF, 1993), here described as annual mean residence times. The values are modified by not presenting data for those boxes where flushing times for more than one year are given by ICES (1983). In general the values are much larger than those calculated from our study. Especially the boxes 7B and 3B exhibit values several factors higher than turn-over times derived from our calculations and Backhaus (1984). The values for box 1 are about a factor 4 and the boxes 2 and 5B are about a factor 2 higher than the corresponding mean values from the gridded model. These results clearly demonstrate that the atmospheric variability and its consequences on the flow induced time scales are definitely below the estimates given in the ICES report (1983). Also note, that in our calculation all inflowing transports, which may vary significantly in their direction, contribute to the flushing time. This effect additionally reduces the flushing time estimates.

The values for the flushing times from the model study by Prandle (1984) are generally higher than those from the present model study or the ones by Backhaus (1984). The reason for the differences are given in the North Sea Quality Status report (NSTF, 1993) by the use of a climatic wind forcing and differences in the resolution of the vertical structure. Prandle (1984) used a 3-monthly constant wind forcing and a 2-D vertically integrated model, two factors responsible for a strong reduction of variability which, as for the ICES estimates, again results in longer flushing times. The use of only one year of calculation, as also suggested by the North Sea Quality Status report (1993), does not lead to these big differences as the comparison of the Backhaus (1984) study for 181 days with our calculations covering 11 years of simulation has demonstrated. It is surprising that Prandle's model setup and the forcing of the model has lead to flushing time estimates which are even higher than the corresponding ICES (1983) values from observation, like for the boxes 1, 2 and 6.

4.3. Advective transport through the ICES boxes

In order to aquire information on the circulation pattern of the North Sea, Fig. 2 presents the advective net transports accross each box boundary in $km^3\ day^{-1}$ derived from 11 years of simulation. The largest inflow and outflow into and out of the North Sea occur at the northern boundary through the deeper boxes. Averaged over 11 years of simulation an amount of $118.4\ km^3\ day^{-1}$ of Atlantic water is introduced into the northern North Sea via the boxes 1, 2 and 7A. About $102.3\ km^3\ day^{-1}$ or 86.4% of these Atlantic water masses recirculate north of the Doggerbank to rejoin the Atlantic via the Norwegian Trench (box 6) at the eastern boundary of the North Sea basin. Of the total North Atlantic inflow about 27.9% influence the central North Sea, here defined as inflow into box 7A. A fraction of only about 4.6% of the northern inflowing Atlantic water masses contribute to the exchange and flushing of water in the southern parts of the North Sea, defined as inflow into box 3B. This inflow is concentrated in the western part of the central North Sea. Here about $2.1\ km^3\ day^{-1}$ of water from the north flow south along the British coast within box 3A, combines with a net contribution from the central North Sea box 7A of $3.4\ km^3\ day^{-1}$ and flow into the English coastal box 3B. From this net inflow into box 3B about $5.3\ km^3\ day^{-1}$ finally enter the Continental coastal area in box 4. Therefore the small contribution of about 4.6 % of the north Atlantic inflow which finally enters the Continental coastal box 4 is still more than the direct inflow into this box via the English Channel with $5.1\ km^3\ day^{-1}$. The southern circulation system adds to the northern outflow with the transport of $21.9\ km^3\ day^{-1}$ going from the Danish coastal box 5B into the Norwegian Trench box 3. This is about twice as much as the inflow form the Baltic and 17.6 % of the total outflow of the Norwegian trench box into the North Atlantic of $134\ km^3\ day^{-1}$.

One has to note that the circulation pattern described for the ICES boxes can not be compared with single measurements. Even a big measuring program like JONSDAP '76 was restricted towards the description of a specific meteorological situation, i.e., "persistent wind" events (Riepma, 1980) which lasted several days at the most. In contrast the circulation pattern described in Fig. 2 show the mean circulation derived from 11 years of simulation. One could of course analyse similar "persistent wind" events extracted from the 11 years of simulation, but this would be beyond the scope of this paper. However the findings by Riepma (1980) and Furnes and Saelen (1977), that the day to day variability of the

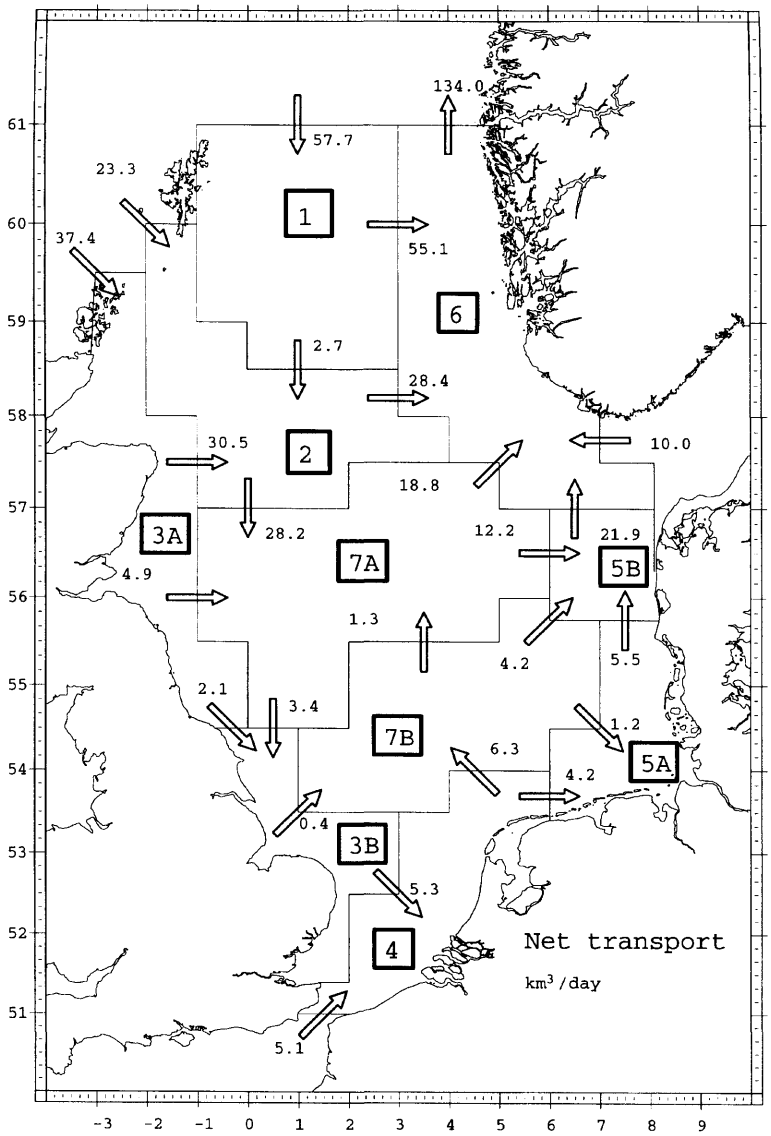

Fig. 2. Horizontal net transport for the ICES boxes ($km^3\ day^{-1}$) derived as annual mean from 11 years of simulation.

transport can be considerably greater than the mean is consistent with our calculations for the in- and outflow time series for the boxes. Basically this agreement is related to the high-frequent wind forcing within the 3-D hydrodynamical model.

For a comparison of Fig. 2 with the transports between the boxes presented in the flushing time report (ICES, 1983) the values given in Sverdrup were recalculated in $km^3\ day^{-1}$. The strongest mismatch between the transports given by ICES (1983) and our horizontal transports occur in the outflow of the Norwegian Trench (box 6). ICES gives a value for the outflow of 69.1 $km^3\ day^{-1}$ and an inflow of 60.4 $km^3\ day^{-1}$, resulting in a net transport out of box 6 of only 8.6 $km^3\ day^{-1}$ in comparison to our value of 134.0 $km^3\ day^{-1}$.

The North Atlantic inflow into box 1 (51.8 km^3 day^{-1}) and box 2 (25.9 km^3 day^{-1}) correspond well with the calculations from the gridded model results. However, the inflow into the Scottish coastal box 3A with 2.5 km^3 day^{-1} is much too low compared to 37.4 km^3 day^{-1} as shown in Fig. 2. There is a strong overestimate in the ICES values for the English Channel inflow given as 12.9 km^3 day^{-1}, which is about a factor 2 higher than the 5.1 km^3 day^{-1} we calculate. Consequently the inflow of 10.3 km^3 day^{-1} into box 5A, which is not affected by the modification of box 5 in our presentation, exceeds our value of 4.2 km^3 day^{-1} in Fig. 2 by the same amount. Unfortunately there is no value given by ICES (1983) for the transport from box 5B into 6, but a strong transport of 15.5 km^3 day^{-1} goes from box 5 into an additional Skagerrak box representing the Juetland Current. This inflow into the Skagerrak box is partly recirculated via the inflow into the Norwegian Trench box 6 of 86.4 km^3 day^{-1}. With an outflow of 69.1 km^3 day^{-1} this results in a net flow into box 6 of 17.2 km^3 day^{-1}, compared to 10.0 km^3 day^{-1} calculated from the gridded model results. Surprising is the uniform flow of 0.86 km^3 day^{-1} away from the British coast (box 3A into 7A, 3B into 7B and 4), whereas our calculations give ranges between 0.4 and 5.3 km^3 day^{-1}. ICES gives no net flow from box 7A into 3B which allows for a contribution of Atlantic water into the southern circulation system. However, there is a contribution of 0.86 km^3 day^{-1} southward from box 7A into box 7B, while our calculations reveal a net transport of 1.3 km^3 day^{-1} northward from box 7B into 7A.

4.4. Horizontal diffusion through the ICES boxes

The horizontal diffusion was calculated by means of eq. (1) from the dispersion model. Subsequently the A_h values were integrated over all gridpoints within each box boundary. Fig. 3 presents the horizontal diffusion rate A_h between adjacent ICES boxes as the mean of 11 years of simulation. Highest A_h rates are found in areas with extensive tidal mixing, namely the Fair Isle Passage with values of 1170.2 and 1151.7 m^2 s^{-1}. In comparison to the Shetland Channel with a small value of 188 m^2 s^{-1} a high value of 775.8 m^2 s^{-1} can be observed for the English Channel. Generally high values are found in the Southern and German Bight and along the English east coast. Here maximum A_h rates between 587.6 and 352.0 m^2 s^{-1} occur. In off-coastal regions, where the tidal mixing activity is smaller, namely in the central and northeastern North Sea, horizontal diffusion rates are significantly lower. Minimum values of about 17.0 m^2 s^{-1} are found in the Norwegian Trench area, while A_h rates between central boxes vary from 97.0 to 32.6 m^2 s^{-1}. From the model study by Prandle (1984) the values for the horizontal dispersion coefficient vary between 1000 m^2 s^{-1} in the English Channel, 300 m^2 s^{-1} for the southern North Sea including the German Bight and the English east coast and 50 m^2 s^{-1} for the central North Sea. Pingree et al. (1975) obtained a similar value for the English Channel, whereas Schott (1966) gave an estimate of 100 m^2 s^{-1} for the southern North Sea. This indicates that the A_h-values of this study lie well in the range determined by other authors.

5. Properties of the ICES boxes derived by integrating the gridded model results over the entire box

In this chapter, the individual properties of the boxes that have to be taken as homogenous within a box model approach will be highlighted. ERSEM needs to pay special attention to the upper mixed layer because this can be seen as roughly equivalent to the biologically productive euphotic zone. According to this, the boxes of the central and northern North Sea, where thermal stratification was assumed to occur regularly in summer were divided vertically in the box setup of the ecosystem model. These boxes were derived from literature (e.g., Fig.14.2 of Becker, 1981). The average depth of the thermocline, averaged over the North Sea and the season, was estimated to be about 30 m and therefore a 'thermocline interface' was introduced at that depth. Keeping in mind that this is a coarse representation of the vertical structure which can not represent, e.g., the deepening of the thermocline during the summer periods, the information provided by the gridded model was used to represent the internal properties of the boxes.

Therefore, at each surface point of the gridded model, the water column is looked at and sub-

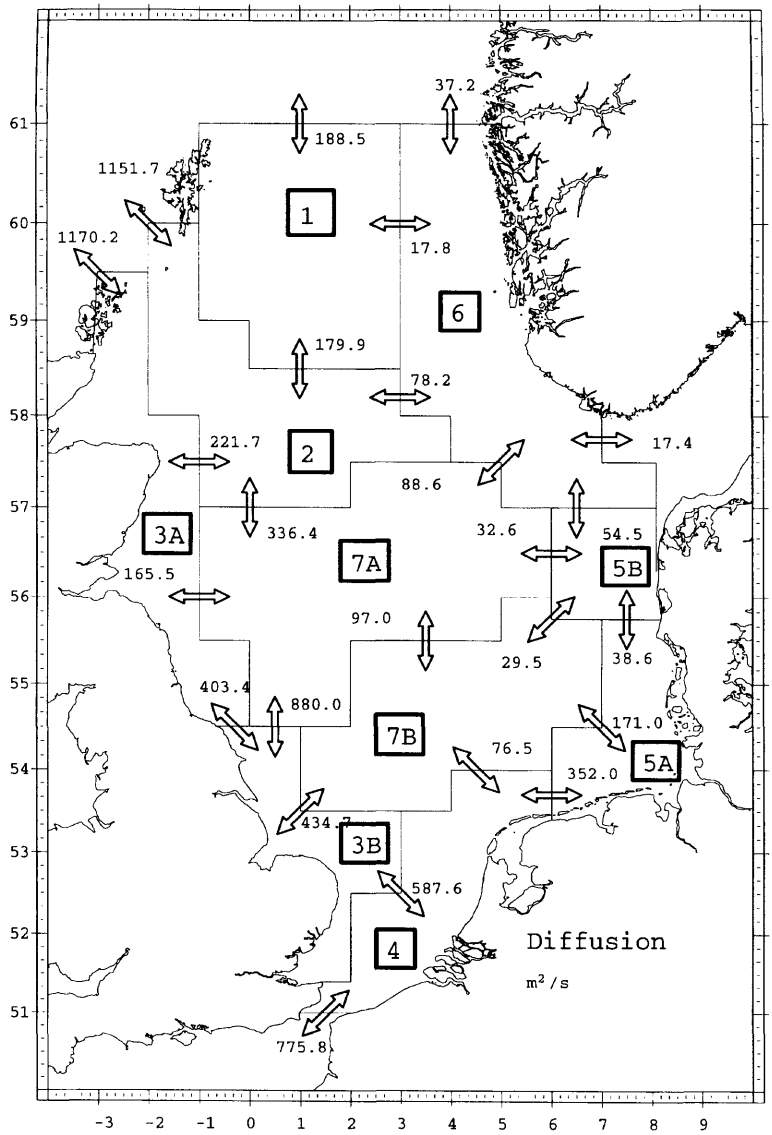

Fig. 3. Horizontal diffusion for the ICES boxes ($m^2\ s^{-1}$) derived as annual mean from 11 years of simulation.

sequently information on the vertical is integrated over the box.

5.1. *Time of occurrence and depth of the thermocline*

Fig. 4a shows the depth of the thermocline in form of two time series for the northern North Sea box 2. The first one (bold line) gives the depth where the maximum temperature gradient of 0.15 °C occurs. This curve starts in the middle of May at about 22 m and remains at a slightly lesser depth till the end of July. Afterwards it increases steadily towards 45 m depth at the end of October where it finally disappears. The second curve (thin line) is derived from the daily values of vertical

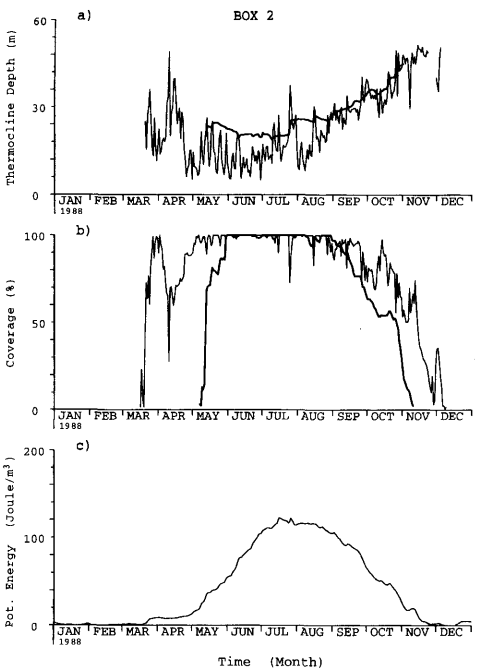

Fig. 4. Information on the vertical structure for the northern North Sea box 2 presented as time series of: (a) the thermocline depth (m) derived by temperature gradient (bold line) and A_v-minimum calculations (thin line); (b) coverage by the thermocline in percent derived by temperature gradient (bold line) and A_v-minimum calculations (thin line); (c) the potential energy (J m^{-3}).

eddy viscosity (A_v), defining the mixed layer depth by a gradient of 0.0134 cm^2 s^{-1} (Pohlmann, 1996b). This curve starts earlier in the middle of March and shows a higher variability. The latter is due to the fact that the A_v values react more sensitively to single wind events whereas the temperature can be seen as a property which integrates fluxes over time. Comparing both curves from May on one sees that the A_v-derived curve generally shows a smaller thermocline depth with only the maximum values touching the temperature-derived curve. However, from August on the fluctuations of the A_v-derived curve become smaller and the two curves coincide quite well.

Both calculations for the thermocline depth and the mixed layer depth were carried out while taking a 20% coverage as a threshold level for the appearance of a thermocline in the respective box. In Fig. 4b the fractional coverage for the two different methods are shown, expressing how many of the 129 model water columns within box 2 are covered by a thermocline using the two different definitions mentioned above. Again one can observe the A_v-derived values to fluctuate more than the temperature-derived ones. Especially at the onset of the thermocline before May, the strong deepening of the thermocline of the A_v-derived values corresponds well with a drastic decrease in the coverage of these values.

Since the temperature-derived curve of the coverage reveals a well defined period of stratification, one can easily compare the duration of the thermocline for the years 1988 and 1989, as listed in Table 3.

Calculated by the temperature gradient the only box with no stratification in both years is the English coastal box 3B. The boxes of the northern and central North Sea reveal values above 160 days of stratification in both years. For the southern central North Sea box 7B the stratification lasts 120 days in 1988 and 143 days in 1989. The Dutch coastal box 4 exhibits only short stratification periods of up to two weeks starting in May whereas the German Bight box 5A has two (1988) and three (1989) week periods from May to July. In contrast the Scottish coastal box 3A and the Danish coastal box 5B show extensive periods of stratification in both years. In 1988 the box 3A exceeds the stratification period of the southern central box 7B by about a month. Generally the stratification in 1988 started about a week later in 1989 and did not last as long in 1989. The central boxes 7A and 7B are the exception here, in 7B the stratification lasted longer in 1989 and in 7A it also started earlier than the year before.

Estimates for the thermal stratification were given by Reid et al. (1988) based on data from Tomczak and Goedecke (1962), taken at the position nearest to the centre of each box. Since the thermal dynamics of the years 1988 and 1989 are well within the range of 11 years of simulations it seems justified to compare those 2 years against the climatological data used in the paper by Reid et al. (1988), especially since the comparison was only meant to be on a qualitative basis. The conclusion that box 3B and 4 remain thermally mixed throughout the year can be supported by the corresponding values in Table 3. According to Reid et al. (1988) the boxes 3A and 5 develop a thermal stratification only to a minor extent and all the remaining boxes show stratification

Table 3. *Occurrence of the thermocline derived from the temperature gradient from the present model for 1988 and 1989*

	1988			1989		
ICES box	begin (date)	end (date)	duration (days)	begin (date)	end (date)	duration (days)
1	10 May	21 Oct.	165	19 May	11 Oct.	146
2	13 May	1 Nov.	173	17 May	27 Oct.	164
6	5 May	26 Oct.	175	11 May	29 Oct.	172
7A	9 May	27 Oct.	172	7 May	2 Nov.	180
7B	5 May	1 Sep.	120	8 May	27 Sep.	143
3A	3 May	5 Oct.	156	17 May	24 Sep.	131
3B	–	–	–	–	–	–
4	24 June	31 June	8	20 May	26 May	7
4				9 June	29 June	21
5A	22 May	4 June	14	21 May	31 May	11
5A	7 June	31 June	25	7 June	31 June	25
5A				4 July	11 July	8
5B	3 May	29 July	89	15 May	2 Sep.	111

between June to November. Because of the modification of box 5 the values of box 5A and 5B in Table 3 can not be compared but for box 3A the stratification period range between 156 days in 1988 and 131 days in 1989. For all the other boxes the stratification period lasts from May to October.

5.2. *Potential energy*

By using the temperature and salinity information from the gridded model, the potential energy PE per unit volume according to Simpson et al. (1977) can be calculated as:

$$\mathrm{PE} = \frac{1}{H}\int_{-H}^{0} (\rho(z) - \bar{\rho})\, gz\,\mathrm{d}z, \qquad (2)$$

with

$$\bar{\rho} = \frac{1}{H}\int_{-H}^{0} \rho(z)\,\mathrm{d}z, \qquad (3)$$

where z is the vertical coordinate (positive upwards), H is the depth, $\rho(z)$ is the density at depth z, with the mean density $\bar{\rho}$ according to eq. (3), and g is the gravitational acceleration. Potential energy per unit volume can be interpreted as the work necessary to redistribute the mass to bring about complete vertical mixing (Reid et al., 1988). One should note that this interpretation implies positive values for potential energy which destroys stratification and therefore increases the potential energy of the water column by the same amount.

Fig. 4c shows the time series of the daily values of the potential energy PE calculated averaged over the northern North Sea box 2. The curve shows a seasonal pattern, with low values in the beginning and at the end of the year. Starting in April the curve of the potential energy begins to increase, reaching its peak in July and August with values up to 122 J m^{-3}. With values above 30 J m^{-3} stratification (Reid et al., 1988) is assumed. For box 2 a thermal stratification during the summer months starting in May and lasting till the end of October is observable. Since the salinity in the Norwegian Trench box 6 (not shown here) plays an important role for the determination of the density, the potential energy reaches very high values up to 479 J m^{-3} at the end of July with a minimum in mid February of about 170 J m^{-3}, clearly representing the dominance of the haline stratification in this part of the North Sea.

In Table 4, this exception of the Norwegian Trench box 6 is indicated by the fact, that stratification lasts the whole year both for 1988 and 1989. Here the permanent halocline is clearly represented in the potential energy calculations. The other strong difference in comparison to the temperature-derived stratification periods

Table 4. *Occurrence of the thermocline derived from potential energy from the present model for 1988 and 1989*

	1988			1989		
ICES box	begin (date)	end (date)	duration (days)	begin (date)	end (date)	duration (days)
1	4 May	5 Nov.	186	22 April	15 Nov.	208
2	13 May	31 Oct.	172	16 May	23 Oct.	161
6	1 Jan	31 Dec.	366	1 Jan	31 Dec.	365
7A	12 May	20 Oct.	162	17 May	27 Oct.	164
7B	24 May	26 July	65	23 May	11 Aug.	81
3A	26 June	22 Sep.	120	5 June	14 Sep.	102
3B	–	–	–	–	–	–
4	–	–	–	–	–	–
5A	–	–	–	–	–	–
5B	28 May	10 July	45	28 May	13 July	48
5B	19 July	23 July	5	19 July	27 July	9

(Table 3) is the lack of stratification within the coastal boxes 3A, 4 and 5A whereas the Danish coastal box 5B shows a major stratification period lasting for at least 45 days from the end of May till the middle of July. After a short break, another period of about 5 (1988) or 9 (1989) days follows. This pattern is the same for both years. The potential energy calculations define much shorter stratification periods for the German Bight box 5B and the Scottish coastal box 3A than the ones derived from the temperature gradient (Table 3). Shorter periods are also derived for the northern or central North Sea boxes 2, 7A and 7B. However, for the northern box 1 which has an external boundary to the North Atlantic, the potential energy calculations lead to much longer stratification periods. This is a result of the salinity structure in the inflowing North Atlantic water. Generally the differences between the years are not as pronounced as for the temperature-derived stratification periods. This results from the smaller inter-annual variability of the salinity distribution which is strongly influencing the density and therefore the potential energy.

The findings by Reid et al. (1988) that also box 4 and 5 show haline stratification, based on the freshwater runoff entering the coastal region, can not be supported by the values given in Table 4.

6. The ERSEM model

ERSEM is an ecosystem model which simulates the ecosystem dynamics in the various regions of the North Sea (Baretta et al., 1995). This comprehensive ecosystem model simulates the large-scale cycling of organic carbon, oxygen and the macro-nutrients N, P and Si over the seasonal cycle in the North Sea. It simulates the pelagic biota of phytoplankton and zooplankton, using estimates of fish predation to effect a predation closure. In addition the chemical transformation of carbon and the macro-nutrients in the benthic system are simulated as well as the biota involved in the benthos. The forcing for the biological part of the model is applied by daily solar radiation and by river inflow of nutrients and particulate matter as provided by the North Sea Task Force modelling workshop (RWS, 1992).

Since the ICES boxes are frequently used for presenting aggregated data for the North Sea, the intention was to build the model on a spatial structure which allows for easy comparison with data as well as a sensible representation of the North Sea subregions. Because the ICES boxes were defined according to morphological, hydrographic and biological aspects of the North Sea, these boxes form a crude but sensible partition of the North Sea. In addition, the computational costs of such a complex model as well as the feasibility to check hundreds of fluxes between different submodules made it advisable to start with reproducing only the gross features of the North Sea.

However, these regions are not independent of each other but are connected by transport mech-

anisms. Advective and diffusive transport of water, abiotic and biotic substances play an important role in shelf seas like the North Sea. The physical flow fields simulated by the 3-D model by Pohlmann (1991) were used to drive the transport forcing for the ecosystem model, with no feedback from the biology to the hydrodynamics. Since the transport influences the spatial distribution of the macro-nutrients, phytoplankton and zooplankton as well as of particulate matter and bacteria it plays an important role within the pelagic part of the ecosystem model. As will be highlighted later, especially the vertical processes are dominant, e.g., in making nutrients available during stratification periods in summer. The details of how the 3-D simulation results have been integrated for the boxes and applied to ERSEM, as well as intrinsic problems of this coupling, have been presented in Lenhart et al., (1995).

6.1. 3-D dispersion model versus ERSEM box model: horizontal advection and diffusion for a point source

In order to judge the transport of substances within the ERSEM box model a scenario was set up in which the results from the box model can be compared with results from the fully 3-D resolving dispersion model. Within this scenario a time series of freshwater discharge covering a one year period for the rivers Rhine and Meuse, as provided by the North Sea Task Force modelling workshop (RWS, 1992), was used as conservative tracer, released from a point source. The dispersion model was run for the year 1988, using the same forcing from the hydrodynamical model as ERSEM. In ERSEM the freshwater was treated as a prognostic variable with only the physical transport processes acting.

The spreading of the freshwater from the point source of the dispersion model can be observed in the upper layer (0–5 m) from Fig. 5 for (a) the 15 July, (b) the 1 September and (c) the 1 October 1988. The isoline representation shows the percentage of freshwater, calculated as the amount of freshwater introduced in m^3 divided by the volume of each grid cell, also in m^3, times 10^2.

In Fig. 5a, one can see a nearly radial spreading of the tracer around the point source within the Dutch coastal box 4. This means that after half a year of simulation hardly any tracer substance has left the area of the box where the tracer was introduced. Only the isoline representing 1 percent of freshwater has approached the German coastal box 5A and the southern North Sea box 7B. On the 1 September (Fig. 5b) the isolines are stretched along the coast in the direction of the Continental coastal current, with higher percentages of freshwater spreading nearly parallel to the coast into the downstream box 5A. Only the isolines representing 1 and 2% of freshwater extend towards the central North Sea and therefore reach box 7B. The picture for the 1st October (Fig. 5c) shows a much wider area covered by the isolines representing 1 and 2% freshwater with higher values missing, except for a small area nearshore of the German Bight box 5A and in the vicinity of the western boundary. On the other hand there is still an area near the Frisian coast with less than 1 percent freshwater, indicating that the German Bight box 5A is not yet completely filled by this low freshwater concentration. It is interesting to note that the isolines representing 2% cover a great part of box 5A but touches only a small area of the adjacent box 7B.

The results of the dispersion model simulation were stored on a daily basis for all grid cells of the model domain. Afterwards, mean, volume weighted, box concentrations were calculated representing %s of freshwater per box volume. Accordingly, ERSEM was run using the same hydrodynamical forcing and the same freshwater inflow as a point source, but with no biological or chemical reaction terms influencing the tracer state variable. Therefore both models take into consideration only physical forcing acting on the tracer.

In order to find the best representation of the ERSEM transport of substances within the box structure compared to the 3-D dispersion model, three different transport parameterizations were used. The first one (Gross) uses the in- and outflow in the form of horizontal advective transport but without horizontal diffusion. The second one (Net) uses only the net transport, whereas the third parameterization used net transport plus horizontal diffusion. For the last parameterization (Net+hDif), the horizontal diffusion coefficients A_h were integrated from the gridded model for each box boundary and implemented in ERSEM as horizontal diffusive flux of a concentration (hDifC):

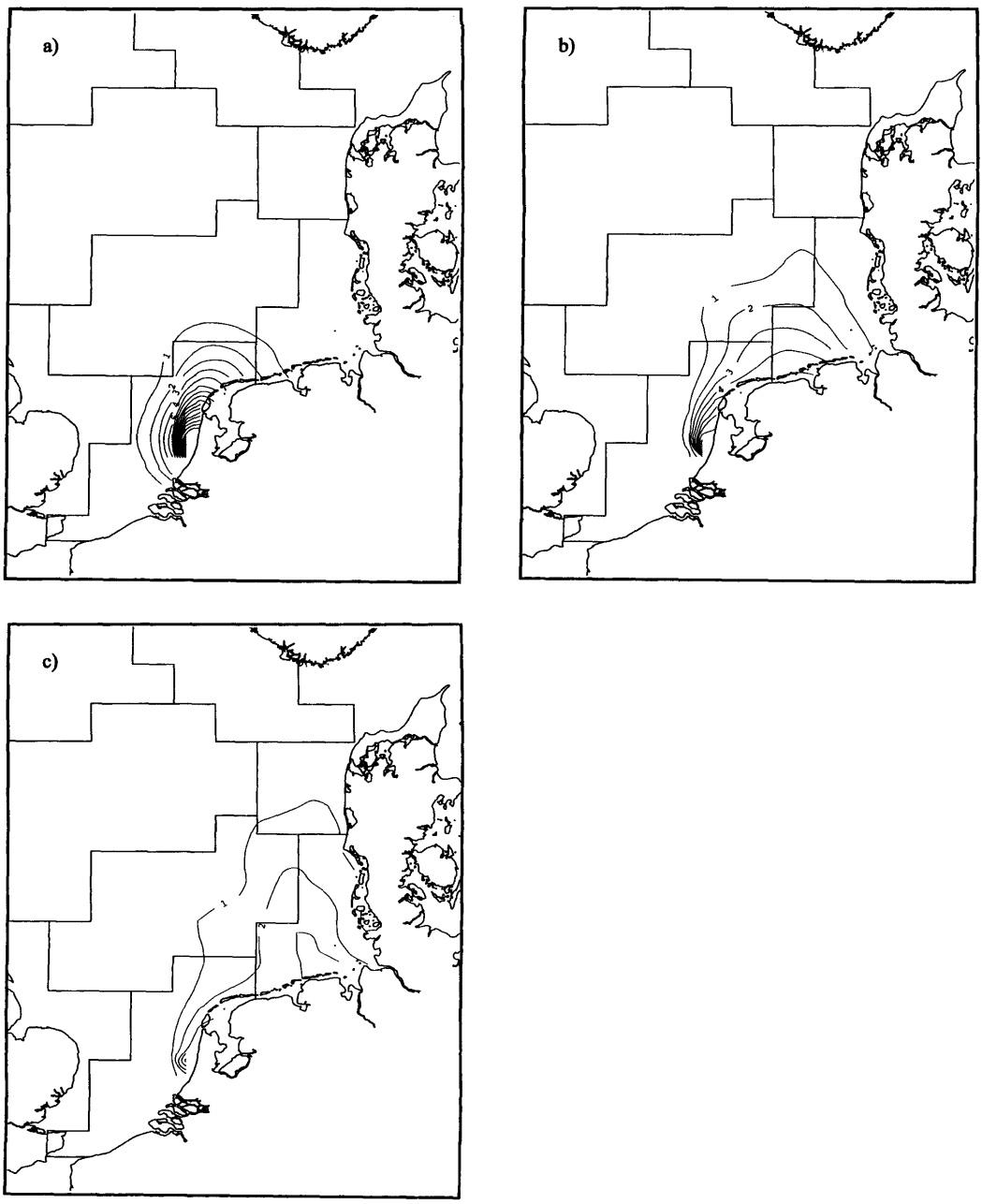

Fig. 5. Isoline representation for the spreading of freshwater from a point source for the 0–5 m layer of the 3-D dispersion model in percent of freshwater for: (a) 15 July; (b) 1 September; (c) 1 October. In addition, the ICES boxes for the North Sea are outlined.

$$\text{hDifC} = A_h \frac{\Delta C}{L_h} F, \tag{4}$$

where ΔC defines the concentration gradient between two adjacent boxes separated by the box boundary of the area F for which A_h is derived. According to the different shapes of the ICES boxes a problem arises by the definition of the horizontal diffusive length scale L_h. In our present study a length of 2 times the length of the grid cell was chosen ($L_h = 2\,\Delta x$).

Fig. 6a shows a comparison of the amount of tracer substance integrated over all the boxes of the model domain and summed up for every day for the dispersion model and the 3 different parameterizations of ERSEM. Therefore the percentage of freshwater is related to the North Sea volume. In addition the total percentage of freshwater (bold line/total) introduced into the model domain cumulative over time is presented. This curve marks the maximum amount of tracer substance that can be found within the system. The dispersion model (thin line) follows this curve till the end of July. Afterwards lower values indicate that a growing part of the tracer has reached the external boundaries of the model area. From 58.4 km^3 freshwater released as tracer from the point source about 0.112% of the North Sea volume or 45.8 km^3 is kept within the model area at the end of the year by the dispersion model.

As one can see all the ERSEM representations give lower values from February onwards, and reach different levels towards the end of the simulation. The lowest level is produced by the representation with the gross transport (Gross, 0.086 percent or 35.13 km^3), followed by the one using net transport in combination with horizontal diffusion (Net + hDif, 0.105% or 42.7 km^3). Only the net transport reaches the level of the gridded dispersion model. The time series for the net transport shows lower values from March on, levels off with the values of the dispersion model by the end of September and finally reaches a slightly higher amount of tracer substance at the end of the year (Net, 0.116 percent or 47.2 km^3). Therefore it was concluded that the numerical diffusion in the box model, resulting from the homogeneity assumption for every box, is so strong that only the least diffusive algorithm, the net transport without any additional horizontal

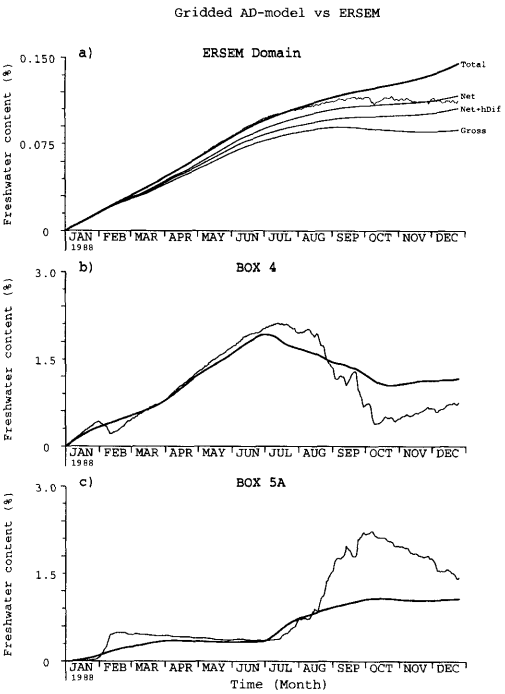

Fig. 6. Comparison from the freshwater tracer study between the 3-D dispersion model and ERSEM, both using the same physical forcing. (a) Cumulative time series as a % of freshwater tracer in relation to the North Sea volume for: (Total) the total amount of tracer in the system, ERSEM parameterizations using: (Net) net advective transport only, (Net + hDif) net transport plus horizontal diffusion, (Gros) gros transport using in- and outflow information at the same time and (thin line) the integrated results of the 3-D dispersion model. Daily time series of % of freshwater in relation to the box volume. Comparison of the results from the ERSEM model (bold line) with the integrated results from the 3-D dispersion model (thin line) for: (b) the Dutch coastal box 4; (c) the German Bight box 5A.

diffusion, could be applied in order to simulate the transport processes correctly. Thus the following graphs (Fig. 6b and c) comparing the percentage of freshwater within a single box integrated over the grid cells of that box from the dispersion simulation results (thin line) with that from ERSEM (bold line), use only the net transport representation for the box model.

The freshwater point source was introduced into the Dutch coastal box 4, where consequently the highest % of freshwater related to the box volume can be observed (Fig. 6b). The box model

predicts a rise of the percentage until the end of June, keeps at lower values for July and August and afterwards remains on a higher level till the end of the year. This rise in the percentage until the end of June corresponds with the nearly radial spreading around the point source in the isoline presentation (Fig. 5a). The drop in percentage afterwards also corresponds with the spreading of the isolines over larger areas (Fig. 5b, c), reflecting an extensive flushing of box 4 during this time of the year.

In Fig. 6c for the German Bight box 5A, the box downstream of box 4, the main features are sharp rises in the percentage calculated from the results of the dispersion model run. The first increase in the percentage of box 5A in the beginning of February is related to a change against the zero background level since the point source is building up a concentration within box 4 first. When a small amount of freshwater is passing the artificial box boundary into box 5A for the first time this causes a steep rise in the percentage of this box. After this first rise, the % of freshwater remains nearly constant with a tendency to become lower reflecting a dilution of the freshwater which has reached the box 5 after the first inflow event. Finally, when the water from box 4, which was enriched with freshwater during the summer stagnation period, passes the boundary into box 5A around August, again a sharp rise in the percentage of freshwater can be observed. The ERSEM box model of course can not reproduce these strong gradients within the time series and therefore yields a much smoother curve which underestimates the high percentages from September onwards.

One has to note that this scenario is designed to test the full capability of a box model using the ICES boxes as basic box structures. Therefore, an extreme high gradient has been applied which can hardly be resolved properly with the strong numerical diffusion at work in this coarse box structure. For ERSEM it has been shown (Lenhart et al., 1995) that for substances like macro-nutrients the horizontal gradients are by far not as extreme as those in the present scenario, e.g., by the use of a zero background concentration. However, from this present scenario the net transport appears to be the appropriate representation for the transport in ERSEM and was therefore introduced in later model versions. This implies that when using boxes of the size of the ICES boxes one has to take into account a considerable numerical diffusion.

6.2. *Influence of vertical diffusion on the ERSEM nutrient dynamics*

The vertical diffusion acting in the 30 m thermocline layer introduces a strong physical signal within the pelagic biota. Even though the vertical diffusion is much weaker than the horizontal advective transport, the strong vertical gradients of nutrients cause pronounced effects in the biochemical environment. In Fig. 7 the effects of the vertical diffusion can be followed up from phosphate to zooplankton. In Fig. 7a, the time series of the vertical diffusion coefficients are shown for the Norwegian trench box 6 for the year 1989

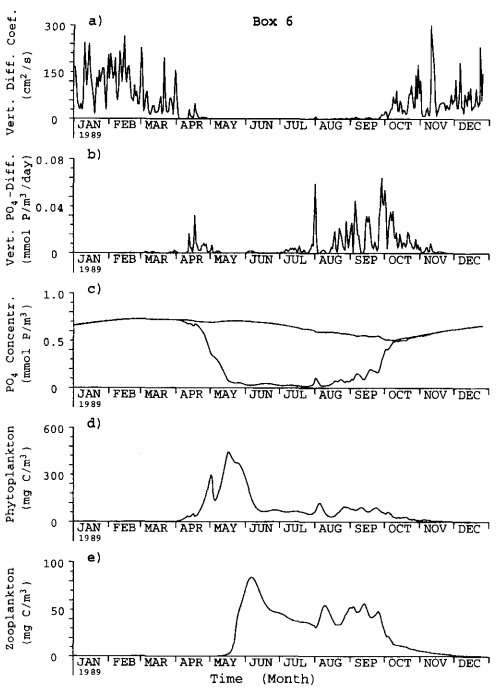

Fig. 7. Daily time series for the Norwegian Trench box 6 for the year 1989, presenting: (a) the vertical diffusion coefficient at 30 m ($cm^2\ s^{-1}$), (b) the vertical PO_4-diffusion into the upper layer (0–30 m) at the 30 m interface (mmol P m^{-3} day^{-1}), (c) the PO_4 concentration for the upper layer (0–30 m) and the lower layer (30 m – bottom) in (mmol P m^{-3}), (d) the phytoplankton concentration (mg C m^{-3}) and (e) the zooplankton concentration (mg C m^{-3}).

in $cm^2\ s^{-1}$. These vertical diffusion coefficients were calculated at the 30 m thermocline interface separating an upper and a lower box. The time series show typical seasonal characteristics with low values during the summer period, lasting from April to the end of September. The vertical diffusive flux of a nutrient like phosphate (PO_4) is determined by the gradient between the upper and lower box. The vertical diffusive flux of a concentration C (vDifC) is calculated in the following way:

$$\text{vDifC} = A_v \frac{\Delta C}{L_v} F, \tag{5}$$

where ΔC defines the concentration gradient between upper and lower box while L_v denotes the vertical diffusive length scale, which is set to 20 m within ERSEM (Lenhart et al., 1995), and F is the area of the thermocline interface. Depending on the gradient ΔC the vertical diffusive flux for the substance C is directed into or out of the upper layer.

The fluxes of phosphate due to vertical diffusion into the upper box are presented in Fig. 7b (mmol P m^{-3} day^{-1}). The corresponding phosphate concentrations for both boxes are shown in Fig. 7c in (mmol P m^{-3}). The lower box shows a high nutrient concentration throughout the year whereas within the upper box a depletion period can be observed from April until September due to nutrient uptake from algae. In Fig. 7d the total phytoplankton concentration as the sum of diatoms and flagellates is presented as time series (mg C m^{-3}). Finally, Fig. 7e shows the corresponding zooplankton concentration (mg C m^{-3}) summed up from those zooplankton state variables for which grazing on phytoplankton is defined in ERSEM.

Even though there are high vertical diffusion coefficients in the beginning and at the end of the year, the corresponding phosphate flux into the upper box is very low. Only when a gradient is developed between the two layers are there flux events into the upper box. These events fade away quickly because of the vertical diffusion coefficient going down to zero during the summer period. Wind events towards the autumn cause high values of the vertical diffusion coefficient again. In combination with a strong nutrient gradient between the two layers due to algae uptake in the upper euphotic layer strong fluxes of phosphate into the upper layer occur which lead to a rise of the concentration in the upper box.

One extreme example can be observed in the beginning of August, where a small peak in the vertical diffusion coefficient in connection with a strong vertical gradient of phosphate between the two layers leads to a strong diffusive flux of phosphate into the upper layer. The effect of this strong flux can be observed in the concentration of phosphate as a peak within the low summer concentration. The result of this peak of nutrient concentration in the euphotic upper layer can be seen as an increase in the total phytoplankton biomass and even in the zooplankton biomass. One should also note the time lag of a few days between the phosphate flux, the rise in the phosphate concentration, the corresponding increase of the total phytoplankton and finally within the zooplankton biomass. The event in August is a major occurence after the summer stagnation where the effect of the nutrient gradient between the boxes can be demonstrated even though the value for the vertical diffusion coefficient is very low. During autumn strong vertical diffusive fluxes of phosphate into the upper box lead to a balance between the phosphate concentration of the boxes by redistributing the phosphate over the water column.

Generally the ERSEM gives a good representation of the nutrient dynamics as long as no strong horizontal gradients are present. On the contrary, the model reacts very sensitively to small changes in the vertical forcing when strong vertical gradients are present, e.g., during the nutrient-limited phase in summer. Thus the local dynamics has been taken into account by introducing a "thermocline layer" at 30 m plus an appropriate parameterization of the vertical diffusion acting at this interface, which makes it possible to represent the biological processes related to the subdivision of the water column.

7. Discussion and conclusions

The properties of the ICES boxes were derived as comprehensive information from the 3-D baroclinic model by Pohlmann (1991). For the 11 years of simulation the water budgets of the boxes could be shown to be well balanced. Calculating the water budget for the whole North Sea results in a

maximum difference between in- and outflow of about ± 0.5 m, related to the surface area, which is in good agreement with other authors (Pohlmann and Sündermann, 1984; Maier-Reimer, 1977). The basin wide mean flushing time was determined to be about 167 days.

The corresponding flushing time values, which range from 2 to 73 days correspond well with a study by Backhaus (1984) based on a similar model setup but a much shorter simulation period. In contrast, the observationally-derived values by ICES (1983) and the model-based values by Prandle (1984) reveal much higher flushing times. Therefore it can be concluded that different model setups, such as the temporal resolution of the forcing as well as the vertical discretisation, lead to a much higher difference in the resulting flushing time than an extension of the period of simulation.

This raises the important question about the comparability of results produced with different forcing fields. Obviously Prandle (1984) was also able to reproduce the dispersion of Caesium correctly using only a spatially homogenous wind stress distribution which was averaged over three months. As he calibrated his model by choosing optimal parameters for the horizontal eddy viscosity formulation, it can be assumed that in his study all the fluctuations with periods smaller than 3 months are parameterized by means of diffusion processes.

The horizontal transport pattern through the boxes reflects 2 major circulation systems, one short recirculation cell in the north fed by the Atlantic inflow and a southern circulation system with an inflow through the English Channel which follows the Continental coast. About 118.4 km^3 d^{-1} of Atlantic water is introduced into the North Sea in the north of which only a mean amount of 4.6% flows south along the British coast, providing a contribution to the southern circulation system. Nevertheless, the inflow of Atlantic water flowing south provides a stronger contribution to the southern circulation system than the direct inflow by the English Channel. A comparison with the ICES report (1983) revealed a strong underestimate of the Norwegian Trench net outflow by a factor 15 whereas the English Channel net inflow was overestimated by a factor 2 within the ICES values. In the same detailed way as for the horizontal transports, the results of the 3-D model did also allow us to determine the horizontal diffusion acting between the boxes, whereas the ICES report (1983) provides estimates for a few boxes only. Generally, the highest rates were found where extensive tidal mixing takes place. Prandle (1984) and Pingree et al. (1984) gave an overestimate for the English Channel with 1000 m^3 s^{-1} in comparison to our value of 775.8 m^2 s^{-1}. However, if we look at the A_h-values for different boundaries between the ICES-boxes, we find that in the central and northern North Sea a pronounced regional variability is present. Since the values provided by Prandle (1984) and Schott (1966) were averaged over these large domains, they only can be used for qualitative comparisons.

The intrinsic properties of the boxes in form of the depth of the thermocline were derived in 2 independent ways, i.e., via the vertical diffusion A_v and via the temperature gradient in the water column. While the deepening of the thermocline during the summer period could clearly be seen for both methods, the A_v-derived curve showed stronger fluctuations refering to single wind events. From the temperature information the period of stratification is calculated for the years 1988 and 1989. The northern and central North Sea boxes generally showed stratification periods of about 160 days, starting in May and lasting until October. For both years the English coastal box 3B showed no stratification, whereas the Scottish box 3A and the Danish box 5B revealed extensive periods of stratification. These findings are in contrast to Reid et al. (1988) who assumed only a minor stratification for box 3A and a stratification period for the central North Sea starting about a month later in June and lasting until November. In addition, stratification periods were estimated based on potential energy calculations. Since the salinity is an important signal for the density in this method, the Norwegian Trench box 6 shows a permanent halocline throughout both years. However, a haline stratification based on freshwater runoff in the Dutch coastal box 4, as assumed by Reid et al. (1988), could not be found. For the northern and central North Sea boxes shorter periods of stratification were estimated by the potential energy calculation in comparison to the temperature-derived estimates. Generally the two methods showed stronger differences than the variation between the two years under consideration.

The estimate of 30 m mixed layer depth as a coarse representation for a stratification within ERSEM was supported by the A_v- and temperature-derived curves for all the boxes. With the exception of box 3A, which is not vertically separated in ERSEM, the determination of stratified boxes by the potential energy calculation gave the same coverage as introduced in the box setup of ERSEM. The stratification in the Scottish box 3A is underestimated for the setup in ERSEM as well as by Reid et al. (1988) in comparison to the calculations based on the gridded model for both methods.

In the last part of the paper a box model based on the modified ICES boxes and forced by the output of the 3-D circulation model has been discussed. Using the tracer simulation of ERSEM, it was possible to compare the results of a box model with results of a fully 3-D dispersion model which was forced with the same 3-D model output as ERSEM. One major feature of the box model is the strong numerical diffusion within these large boxes. The scenario, using freshwater as a conservative tracer being introduced in form of a point source, creates strong horizontal gradients in the vicinity of the inlet. In this investigation, an extreme case study is chosen in order to find an appropriate representation of transport for the box model. Only the net transport, which gives the lowest possible transport rate, could be applied in order to simulate the transport processes correctly in comparison to a 3-D dispersion model. This implies that for the physical forcing of a box model of the size of the ICES boxes it is not necessary to take into account any horizontal diffusion (which could be provided by the 3-D circulation model) because of the strong artificial horizontal diffusion of the advection scheme acting within these coarse boxes.

Therefore one has to consider the horizontal gradients necessary to be resolved in order to decide whether the ICES boxes and the net transport linked to the boxes are the appropriate representation of the features one wants to study. For the attempt in ERSEM to represent the gross features of the North Sea, the horizontal gradients, e.g., for the macro-nutrients are small, and the tests with using gross advective transport as a forcing resulted in only minor deviations from the annual cycles of the simulated nutrient concentrations. Also the option of an easily accessible comparison with aggregated measurements for the boxes as well as the reduced computational costs as a result of the rather small number of boxes have to be considered.

If it is intended to focus on regions with strong horizontal gradients, like the Continental coastal region, one clearly has to reduce the size of the boxes in order to get an appropriate representation. This further step in the development of the ERSEM model is under way, now benefiting from the experience of having started with the coarse structure of the ICES boxes. This implies a new test of the transport representation for these new boxes, which also ought to be choosen under the consideration that horizontal diffusion should be included within the transport representation. This would allow us to fully use the potential of the stored output from the circulation model.

With ERSEM a good example is given of how a modification of the ICES boxes, namely the vertical separation of the deep boxes in the central and northern North Sea, can add a considerable amount of realism by the introduction of the biologically important thermocline. Within this structural setup and only weak vertical advective fluxes (Radach & Lenhart, 1995), the dominant role of the vertical diffusion as the major physical forcing during the nutrient-limited part of the year has clearly be shown. Here the strong vertical gradients allow for intensive nutrient fluxes into the upper boxes even under relatively weak physical forcing conditions. The effect of these fluxes can be followed not only within the nutrient state variable itself but also in the biota, e.g., in the response of the phytoplankton to the change of the nutrient concentration as well as the subsequent response in the zooplankton. One should keep in mind that the introduction of the thermocline interface at 30 m with the corresponding vertical diffusion coefficients is a coarse parameterization of the vertical water column dynamics. However, the resulting nutrient concentrations correspond quite well with the annual cycle in the upper and lower layer of the water column deduced by measurements (Radach & Lenhart, 1995). Moreover, one can observe a close dynamical interaction between the physical forcing and the subsequent reaction of the major state variables of the pelagic part of the ecosystem model ERSEM.

8. Acknowledgements

This research was funded by the German Federal Ministry for Research and Technology (KUSTOS/BMFT-03F0111A) and by the European Community under MAST contract number CT90-0021. The authors are indebted to J. O. Backhaus for making available the original version of the Hamburg Shelf Sea Circulation Model. We like to thank G. Radach for his continuous help and valuable discussions as well as J.W. Baretta, H. Langenberg, W. Kühn, A. Moll and J. Paetsch, whose criticism led to many improvements of the manuscript. Thanks are due to B. Hellmann, A. Hufschmidt and R. Luff for their technical support.

REFERENCES

Backhaus, J. 1983. A semi-implicit scheme for the shallow water equations for application to shelf sea modelling. *Cont. Shelf Res.* **2**, 243–254.

Backhaus, J. 1984. Estimates of the variability of low frequency currents and flushing times of the North Sea. *ICES Hydrography Committee C.M. 1984* **C**, **24**, 1–18.

Backhaus, J. 1985. A Three-Dimensional Model for the Simulation of Shelf Sea Dynamics. *Dt. hydrogr. Z.* **38** (**H5**), 167–262.

Backhaus, J. and Hainbucher, D. 1987. A finite difference general circulation model for the shelf seas and its application to low frequency variability on the North European Shelf. In: *Three-dimensional models of marine and estuarine dynamics* (eds. Nihoul, J.C.J. and Jamart., B.M.). Elsevier Oceanography Series **45**, Amsterdam, 221–244.

Baretta, J. W., Ebenhöh, W. and Ruardij, P. 1995. An overview over the European Reginal Sea Ecosystem Model, a complex marine ecosystem model. *Neth. J. Sea Res.* **33**, 233–246.

Becker, G. 1981. Beiträge zur Hydrographie und Wärmebilanz der Nordsee. (in German), *Dt. hydrogr. Z.* **34**, 167–262.

Becker, G., Frey, H. and Wegner, G. 1984. North Sea surface temperature means 1971 to 1980 and their differences compared with ICES means (1905–1954). *ICES Hydrography Committee C.M. 1984* **C 1**, 34 pp.

Bolin, B. and Rohde, H. 1973. A note on the concepts of age distribution and average transit time in natural reservoirs. *Tellus* **30**, 185–188.

Damm, P. 1989. Klimatologischer Atlas des Salzgehaltes, der Temperatur und der Dichte in der Nordsee, 1968–1985 (in German), *Inst. Meeresk. Univ. Hamburg, Tech. Rep.* **6–89**, 81 pp.

Furnes, G. K. and Saelen, O. H. 1977. Currents and hydrography in the Norwegian Coastal Current off Utsira during JONSDAP '76. *The Norwegian coastal current project.* Report **2/77**, 16 pp.

Hainbucher, D., Pohlmann, T. and Backhaus, J. 1987. Transport of conservative passive tracers in the North Sea: First results of a circulation and transport model. *Cont. Shelf. Res.* **7**, 1161–1179.

Howarth, M. J., Dyer, K. R., Joint, I. R., Hydes, D. J., Purdie, D. A., Edmunds, H., Jones, J. E., Lowry, R. K., Moffat, T. J., Pomroy, A. J. and Proctor, R. 1994. Seasonal cycles and their spatial variability. In: *Understanding the North Sea system* (eds. Charnock, H., Dyer, K. R., Huthnance, J. M., Liss, P. S., Simpson, J. H. and Tett, P. B.). The Royal Society, Chapman and Hall, London: 5–25.

ICES, 1983. Study group on the flushing times of the North Sea. *Coop. Res. Rep.* **123**, 159 pp.

Kochergin, V. P. 1987. Three-dimensional prognostic models. In: *Three-dimensional coastal ocean models* (ed. Heaps, N. S.). Coastal and Estuarine Science 4, Washington, D.C., American Geophysical Union, 201–208.

Kühn, W., Radach, G. and Kersten, M. 1992. Cadmium in the North Sea: a mass balance. *Journal of Marine Sciences* **3**, 209–224.

Laevastu, T. 1963. Surface water types of the North Sea and their characteristics. Serial atlas of the marine environment. American Geograph. Soc., New York. Fol. **4**.

Lenhart, H. J., Radach, G., Backhaus, J. O. and Pohlmann, T. 1995. Simulations of the North Sea circulation, its variability, and its implementation as hydrodynamical forcing in ERSEM. *Neth. J. Sea Res.* **33**, 271–299.

Luthardt, H. 1987. Analyse der wassernahen Druck- und Windfelder über der Nordsee aus Routinebeobachtungen (in German), *Hamburger Geophysikalische Einzelschriften* **A83**, 1–115.

Maier-Reimer, E. 1977. Residual circulation in the North Sea due to M_2-tide and mean annual wind stress. *Dt. Hydrogr. Z.* **30**, 69–80.

Maier-Reimer, E. and Sündermann, J. 1982. On tracer methods in computational hydrodynamics. In: *Engineering applications of computational hydraulics, Vol. 1* (eds. Abbott, M. B. and Cunge, J. A.). Pitman Advanced Publishing Program. Boston, 198–217.

North Sea Task Force, 1993. *North Sea quality status report.* Oslo and Paris Commissions, London, 132 pp.

Pingree, R. D., Pennycuick, L. and Battin, G. A. W. 1975. A time-varying temperature model of mixing in the English Channel. *J. Mar. Biol. Assoc. UK* **55**, 975–992.

Pohlmann, T. 1991. *Untersuchung hydro- und thermodynamischer Prozesse in der Nordsee mit einem dreidimensionalen numerischen Modell.* Dissertation Uni – Hamburg, 116 pp.

Pohlmann, T. 1996a. Predicting the thermocline in a circulation model of the North Sea. Part I: Model

description, calibration, and verification. *Cont. Shelf Res.* **7**, 131–146.

Pohlmann, T. 1996b. Calculating the annual cycle of the vertical eddy viscosity in the North Sea with a three-dimensional baroclinic shelf sea circulation model. *Cont. Shelf Res.* **7**, 147–162.

Pohlmann, T., Backhaus, J.O. and Hainbucher, D. 1987. Validation of a Three-Dimensional Dispersion Model for Cs^{137} in the North European Shelf Sea. *ICES Hydrography Committee C.M. 1987* **C**, **34**, 1–12.

Pohlmann, T. and Sündermann, J. 1994. Sea level rise problems. In: *Engineering risk in the natural resource management* (eds. Duckstein, L. and Parent, E.). NATO ASI Series, Kluwer Academic Publishers, Dordrecht. Series E: Applied Science, vol. 275, 219–234.

Prandle, G. 1984. A model study of the mixing of ^{137}Cs in the seas of the European continental shelf. *Phil. Trans. R. Soc. London* **A310**, 407–436.

Radach, G. 1992. Ecosystem Functioning in the German Bight Under Continental Nutrient Inputs by Rivers. *Estuaries* **15**, 477–496.

Radach, G., Schönfeld, W. and Lenhart, H. J. 1990. Nährstoffe in der Nordsee—Eutrophierung, Hypertrophierung und deren Auswirkungen. (In German), In: *Warnsignale aus der Nordsee* (ed. Lozán, J. L.). Paul Parey Verlag, 48–65.

Radach, G. and Lenhart, H.J. 1995. Nutrient dynamics in the North Sea: Fluxes and budgets in the water derived from ERSEM. *Neth. J. Sea Res.* **33**, 301–335.

Reid, P. C., Taylor, A. H. and Stephens, J. A. 1988. The hydrography and hydrographic balances of the North Sea. In: *Pollution of the North Sea, an assessment* (eds. Salomons, W., Bayne, B. L., Duursma, E. K. and Förster, U.). Springer Verlag, Heidelberg, pp. 3–19.

Riepma, H. W. 1980. Residual currents in the North Sea during IN/OUT phase of JONSDAP '76. First results. *Meteor Forschungsergebnisse* **A22**, 19–32.

Roache, P. J. 1972. On artificial viscosity. *Journal of Computational Physics* **10**, 169–184.

RWS (Rijkswaterstaat) 1992. *Guidance document for the NSTF modelling Workshop*, 6–8 May, 1992. Den Haag: Directoraat Generaal Rijkswaterstaat, 41 pp.

Schott, F. 1966. The surface salinity of the North Sea. *Dt. Hydrogr. Z. Reihe A Erg.* **H8**, 1–58.

Simpson, J. H., Hughes, D. H. and Morris, N. C. G. 1977. The relation of the seasonal stratification to tidal mixing on the continental shelf. In: *A voyage of discovery*. George Deacin 70th anniversary volume (ed. Angel, M. V.) Pergamon, London, 327–340.

Tomczak, G. and Goedecke, E. 1962. Monatskarten der Temperatur der Nordsee, dargestellt für verschiedene Tiefenhorizonte (in German). *Dt. Hydrogr. Z. Erg.* **Z7**, 16 pp.

Van Dam, G. C. 1994. Study of shear dispersion in tidal waters by applying disrete particle techniques. In: *Mixing and transport in the environment* (eds. K. J. Beven, K. J., Chatwin, P. C. and Millbank, J. H.). Wiley and Sons.